Journal Name

ARTICLE

Clayey-sand filter for the pharmaceuticals removal from wastewater effluent: Percolation experiments

Received 00th January 20xx,
Accepted 00th January 20xx

DOI: 10.1039/x0xx00000x

www.rsc.org/

T. Thiebault,*[a] M. Boussafir,[a] R. Guégan,[a] C. Le Milbeau[a] and L. Le Forestier[a]

The objective of the study was to evaluate the sorption of a pool of pharmaceutically active compounds (PhACs) onto a clay-sand filter in a dynamic sorption experiment. The chosen adsorbent should have suitable chemical properties for the removal of the targeted PhACs and also consistent hydrodynamic behavior regarding field application. In this aim, the impact of interfoliar cation (Ca^{2+} or Na^{+}) intercalated into natural montmorillonite (Swy2) was tested by using different clay-sand ratios (from 0% to 100% of clay minerals). Only Ca-Swy2 showed a consistent hydraulic conductivity for field application with a value of 4.78 x 10^{-8} $m.s^{-1}$ for 5%-95% clay-sand ratio. The sorption of PhACs onto this filter was investigated using œdometer cells by varying two parameters, the solution matrix (ultra-pure water or natural effluent) and the injection pressure (0.1 MPa and 0.2 MPa). PhACs were effectively adsorbed onto the filter for each experiment at different levels. The drop in injection pressure was a favorable factor for sorption whatever the matrix, with median global removal of ~45% at 0.2 MPa and ~75% at 0.1 Mpa. The effect of the matrix exhibited two different trends as a function of the molecular charge of each PhAC. While cationic compounds were more effectively sorbed in the ultra-pure water matrix than in effluent matrix the sorption of anionic PhACs was more effective in the effluent matrix than in ultra-pure water. This indicates that the charge of the pollutant is a key parameter controlling the efficiency of the adsorbent. Despite these removal variations, the filter exhibited a significant sorption capacity especially at 0.1 MPa. It can therefore be an efficient solution for the removal of PhACs by tertiary filtration.

Introduction

Emerging Pollutants (EPs) represent a common form of pollution in numerous water compartments, from effluents to drinking water. Pharmaceutically Active Compounds (PhACs) account for more than 3,000 compounds among the most concentrated and persistent ones in the environment.[1,2] They constitute a representative part of EPs due to their wide variety of chemical properties.[3,4]

Ever since the study by Richardson and Bowron highlighting the fate of pharmaceutical residues in the environment,[5] several investigations have been conducted in this field over the last thirty years. Studies have focused on the removal of PhACs in Waste-Water Treatment Plants (WWTPs),[6,7] and on improving the sensitivity of analytical methods in order to better characterize their occurrence in the environment.[8,9]

There are three main types of WWTPs: activated sludge treatment plants, phytoplanted filters or lagoon-based systems, but the removal of EPs remains insufficient for all of them. [10–12] The main consequence of this lack of efficiency is the constant discharge of PhACs into the aquatic system. Even if PhACs are present in natural waters at relatively low concentrations, from several $ng.L^{-1}$ to $\mu g.L^{-1}$,[4,13] their toxicity has been widely proved,[14,15] particularly for endocrine disruptors.[16,17] Moreover, some PhACs can be concentrated in natural beings,[18] and contaminate the whole trophic chain including humans with poorly-known consequences.[19] While this contamination goes beyond issues of human health, it raises awareness of the hazards generated by EPs and particularly PhACs.

Waste-water treatment is framed by two major factors, purification capacity and cost. Numerous innovative methods such as activated carbon or UV-oxidation exhibit excellent results for the removal of EPs but are often reserved for drinking water treatment due to prohibitive costs.[20] In addition, oxidation creates metabolites,[21] whose toxicity is still unknown today.

Ali et al. showed by a simple calculation between several removal techniques that adsorption mechanisms are the most appropriate and easiest way to remove both inorganic and organic micro-pollutants,[22] since the adsorbent material has a large specific surface and a good affinity with the targeted micro-pollutants.[23,24]

[a] Institut des Sciences de la Terre d'Orléans, UMR 7327, Univ Orléans, CNRS, BRGM, 1A Rue de la Férollerie, 45071 Orléans, France. E-mail : thomas.thiebault@cnrs-orleans.fr

† Footnotes relating to the title and/or authors should appear here.

Electronic Supplementary Information (ESI) available: [details of any supplementary information available should be included here]. See DOI: 10.1039/x0xx00000x

Drug	Abbreviation	CAS-Number	M_w	pKa	log K_{ow}	S_w	Charge
Atenolol $C_{14}H_{22}N_2O_3$	ATE	29122-68-7	266.34	9.6	0.16	300	+
Codeine $C_{18}H_{21}NO_3$	COD	76-57-3	299.36	8.21	1.2	79 x 10^2	+
Diazepam $C_{16}H_{13}ClN_2O$	DIA	439-14-5	284.74	3.4	2.82	50	0
Diclofenac $C_{14}H_{11}Cl_2NO_2$	DCF	15307-79-6	296.15	4.15	4.06	50 x 10^3	-
Doxepin $C_{19}H_{21}NO$	DOX	1229-29-4	279.38	8.96	3.86	32 x 10^3	+
Gemfibrozil $C_{15}H_{22}O_3$	GEM	25812-30-0	250.33	4.8	4.33	4.97	-
Ibuprofen $C_{13}H_{18}O_2$	IBU	15687-27-1	206.28	4.91	3.72	21	-
Ketoprofen $C_{16}H_{14}O_3$	KET	22071-15-4	254.28	4.45	2.81	51	-
Metoprolol $C_{15}H_{25}NO_3$	MET	56392-17-7	267.36	9.6	1.79	47 x 10^2	+
Naproxen $C_{14}H_{14}O_3$	NAP	22204-53-1	230.26	4.15	3	15.9	-
Oxazepam $C_{15}H_{11}ClN_2O_2$	OXA	604-75-1	286.97	1.7-11.6	2.31	20.71	0
Progesterone $C_{21}H_{30}O_2$	PRO	57-83-0	314.46	-	4.04	8.81	0
Tramadol $C_{16}H_{25}NO_2$	TRA	27203-92-5	263.37	9.41	2.51	75 x 10^3	+
Trimethoprim $C_{14}H_{18}N_4O_3$	TRI	738-70-5	290.32	7.2	0.38	400	0

With M_w, the molecular weight in g.mol^{-1}, pKa the acid dissociation constant, log K_{ow} the octanol/water partition coefficient, S_w the solubility in water at 25°C in mg.L^{-1} and Charge, the dominant form at pH=7

Table 1: Selected pollutants and parameters used in this work

Natural materials such as clays offer a good balance between reactivity and cost for the treatment of effluents.[25] The efficiency of clays CEC (Cationic Exchange Capacity) in water is well documented.[26–28] After all, numerous PhACs are not in cationic form but in neutral or anionic form in environmental conditions. Another key parameter is the influence of the solid-liquid ratio, which is often very remote from realistic applications.[29,30] The latter two studies sought to gain a better understanding of sorption mechanisms for which starting concentrations are often largely overestimated compared to simulation approaching field conditions. To our knowledge, no study has investigated the sorption of PhACs at low starting concentrations (25 µg.L^{-1}) onto natural clays. However sorption experiments with PhAC concentrations that are as close as possible to those found in natural environments and water purification plants are necessary in order to estimate the efficiency of sand and clay mixtures and the real affinities between the tested materials and the targeted pollutants.

A similar concern also frames the choice of the geosorbents and their characteristics as interlayer cation, which controls the sorption capacity and hydrodynamic behavior.[31,32]

In view of the well-established capacity of clays to remove numerous compounds from water, the present study addressed three main issues: (i) the real capacity of slightly modified clay to treat a complex solution in pure water or effluent (ii) the impact of the kinetic transfer and the matrix effect on the sorption and (iii) the feasibility of a clay-based filter for the removal of PhACs.

Materials and Methods

Filter: clay minerals and sand

The sand used was uniformly fine-grained Fontainebleau quartz sand (from the Paris basin, France) of analytical grade, and with a granulometry of 100-150 MESH.

The clay mineral chosen was Swy2 Wyoming montmorillonite (Crook County Wyoming, United States), supplied by the Source Clays Repository of the Clay Minerals Society. After <2 µm fractionation by gravity sedimentation, the Swy2 sample was Na-exchanged by well-established procedures.[33] This Na-Swy2 was the starting material for the production of Ca-Swy2 with the same procedure, by replacing NaCl with $CaCl_2$. These two interlayer cations were chosen because of their predominance in the environment.

Different proportions of sand and clay were tested to estimate the hydrodynamic properties of the resulting mix, with clay percentage in the filter of 5%, 10%, 50% and 100% (i.e. pure clay) and with a constant total mass of 8.0 ± 0.4g. For percolation tests with PhACs, a 5% clay filter was used.

PhACs and chemical reagents

The 14 PhAC standards (purity grade > 98%; see Table 1 for details) were obtained from Sigma-Aldrich for ATE, COD, DIA, DOX (Doxepin Hydrochloride), GEM, KET, MET (Metoprolol Tartrate salt), NAP, OXA, PRO, TRA (Tramadol Hydrochloride), TRI, and from Acros Organics for DCF (Diclofenac Sodium) and IBU.

Chemical reagents of analytical grade, methanol (MeOH) and pyridine were purchased from Fisher Scientific. N-tert-Butyldimethylsilyl-N-methyltrifluoroacetamide (MTBSTFA, >95%) was supplied by Sigma-Aldrich.

Percolation Experiments

Percolation experiments were carried out in œdometer cells. This specific equipment was developed to understand the hydrodynamic behavior of a solid sample under different conditions.[34]

The œdometer cell (internal diameter = 0.04 m) and the injection syringe were both connected to a distinct compressed-air system in order to apply respectively the mechanical pressure on the sorbent material and the injection pressure on the leaching solution. The equipment scheme and further details are given in Figure S1 and in Gautier et al.[35]

For each experiment, 8 g of material (clay-sand mix) was gradually compacted on the bottom side up to 0.5 MPa, then totally unloaded, and compacted again at a mechanical pressure of 0.3 MPa. The solution was injected at the upper side into this compacted sample at a constant pressure during experiments. The injection pressure is the variable which controls the interaction kinetic between the solution and the material. Indeed, œdometer cells enable physical and hydraulic properties to be jointly controlled. Two different injection pressures were used in this study, 0.1 and 0.2 MPa.

In order to control impact of the matrix on the adsorption of PhACs, two solutions were used in the experiments: (i) a mix, hereafter called S, of each of the 14 selected PhACs at concentrations around 25 µg.L^{-1} in ultra-pure water, and (ii) a mix between the 14 PhACs and an effluent of a French rural WWTP, called N. Although PhACs were present in this effluent their maximum concentration around 200 ng.L^{-1} did not affect our results by modifying starting concentrations noticeably (Table S1 for details, and Table S2 for the chemical parameters of the chosen effluent).

The choice of the starting concentration at 25 µg.L^{-1} for each PhAC corresponds to the maximum PhAC concentrations in some effluents.[13]

During percolation experiments, leachate samples were collected each time that a volume of 100 mL solution passed through the filter. A total of 1 L (10 x 100 mL) was therefore used for each percolation experiment.

Leachate and clay analyses

Leachate analysis

Leachate solutions were concentrated by Solid-Phase Extraction (SPE) and analyzed by Gas Chromatography coupled to Mass Spectrometry (GC-MS).

PhAC extraction was carried out on a 6mL glass cartridge filled with HR-X phase (Macherey-Nagel). Cartridges were conditioned with 5 mL of MeOH then with 5mL of ultra-pure water. Columns were filled with 100 mL of sample and then rinsed with 5 mL of ultra-pure water before drying for 30 minutes under vacuum. Finally, elution was performed with 3 x 5 mL of MeOH. Thereafter, internal standard was added to organic layers, which were evaporated under reduced pressure. Residues were derivatized with MTBSTFA according to Schummer et al.[36]

Analyses were performed on a Trace GC Ultra gas chromatograph (GC) coupled to a TSQ Quantum XLS mass spectrometer equipped with an AS 3000 autosampler (both from Thermo Scientific). The GC was fitted with a Thermo Trace Gold TG-5 MS capillary column (60 m, 0.25 mm i.d., 0.25 µm film thickness).

The temperature of the column was held at 50°C for 3 min, increased from 50 to 120°C at 30°C.min^{-1}, and from 120 to 310°C at 3°C.min^{-1} with a final isothermal hold at 310°C for 21 min. 2 µL of sample was injected in splitless mode at 280°C. Helium was the carrier gas (1 mL.min^{-1}). The mass spectrometer was operated in EI mode at 70 eV, from m/z 50 to 500.

Clay characterization and global carbon analysis

X-ray diffraction (XRD) patterns were recorded between 2 and 64° (2θ) using a Thermo Electron ARL'XTRA diffractometer equipped with a Cu anode (Cu Kα1,2 = 1.5418 Å) coupled with a Si(Li) solid detector. Experimental measurement parameters were 10s counting time per 0.04°2Θ step. The diffractograms were performed with dry powder samples (100 °C for 24 h).

Fourier transform infrared (FTIR) measurements were recorded in the range 650-4000 cm^{-1}, using a Thermo Nicolet 6700 FT spectrometer equipped with a Deuterated Triglycine Sulfate (DTGS) detector and a Nicolet Continuum microscope. The analyses were performed in transmission mode and each spectrum was the average of 256 scans collected at 2 cm^{-1} resolution.

Carbon and nitrogen analyses were performed on powdered samples by using a Thermo Scientific Flash 2000 organic analyzer assuming an analytical error of 0.05%.

Data analysis

To characterize the distribution of a compound between a potential sorbent and the dissolved phase, the Log K_d parameter is often used.[37] The computation corresponding to its calculation is expressed as follows:

$$\log(K_d) = \log(\frac{q_s}{q_e}) \quad (1)$$

with K_d the solid-liquid distribution coefficient (L.kg^{-1}), q_s the sorbed concentration (mg.kg^{-1}) and q_e the equilibrium concentration (mg.L^{-1}).

Statistical tests were performed to verify the significance of some hypothesis using the Student test with a chosen statistical threshold of 0.01 for the resulting *p*-values.

To estimate the link between time and sorption capacity and to describe the sorption dynamic, the first-order Lagergren equation, the second-order kinetics model and the Bangham equations are often used.[38]

These equations are expressed in linear form by equations (2)-(4) respectively:

$$\log(q_m - q_t) = \log q_{\mathrm{m}} - \frac{k_1}{2.303}t \quad (2)$$

$$\frac{t}{q_t} = \frac{1}{k_2 {q_{\mathrm{m}}}^2} + \frac{1}{q_{\mathrm{m}}}t \quad (3)$$

$$\log q_t = \log k_b + \frac{1}{n}\log t \quad (4)$$

with q_t the sorbed concentration in µg.mg^{-1} at the time t (min), q_m the pseudo-equilibrium sorbed concentration (µg.mg^{-1}), k_1 (min^{-1}), k_2 (g.g^{-1}.min^{-1}) and k_b (g.g^{-1}.min^{-1}) respectively the first-order, the second-order and the Bangham sorption rate constants.

Each equation is based on different assumptions:

(i) the first-order Lagergren model considers that the quantity of unoccupied adsorption sites is proportional to the adsorption rate of adsorbate onto adsorption sites

(ii) the second-order kinetic model assumes that the adsorption is chemically accomplished

(iii) The Bangham equation considers a fast velocity of adsorption and a slow attainment of sorption equilibrium

These equations were applied to the experimental results.

Results and discussion

Hydrodynamic properties

Percolation experiments were first performed with water solution in order to determine the hydraulic conductivity (K) of the different clay-sand materials. K, expressed in m.s^{-1}, was calculated from Darcy's law, using the expression developed for a saturated medium:[39]

$$K = \frac{Q}{i.S}$$

where Q is the measured volumetric flow rate (m^3.s^{-1}) at the steady state, i is the hydraulic gradient and S is the cross-sectional area of the œdometer cell (m^2).

For a potential environmental application, the clay-sand filter should have hydrodynamic properties that correspond to the hydraulic conductivities operable in actual treatment installations, whereas clays are a natural barrier used for example to trap nuclear wastes.[40]

Clays	SSA	CEC	ε_{max}	Θ_{max}
Na-Swy2	45.4[a]	85.0±2.7[a]	37%[a]	75%
Ca-Swy2	46.0[b]	85.1±0.01[b]	1.5%	62%

With SSA, Specific Surface Area (m².g^{-1}); CEC, Cationic Exchange Capacity (meq.100g^{-1} of clays); ε_{max}, the maximum axial swelling strain for 100% clay sample; Θ_{max}, the maximum water content for 100% clay sample and [a] 33[b]41

Table 2: Main properties of the selected clays saturated with Na^+ and Ca^{2+} as interfoliar cations

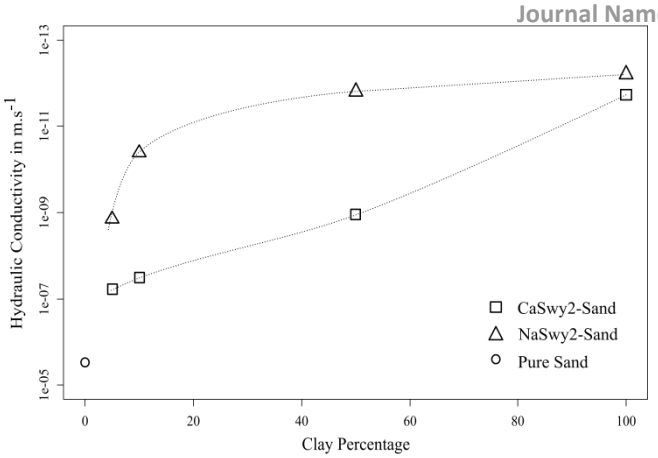

Figure 1: Hydraulic Conductivity as a function of the clay percentage in the clay-sand filter with circle: pure sand, triangles: clay-sand filters with Na-Swy2 and squares: clay-sand filters with Ca-Swy2

This specific application should find a good balance between high permeable Fontainebleau sand and Na- or Ca-Swy2 clay with a low permeability.

Different clay-sand ratios were tested for both Na- and Ca-SWy2 in order to simulate and calculate the maximum flow of solution that can pass through the filter.

In accordance with the aim of this work, the ideal clay-sand ratio should include a low proportion of clay. As expected, the decrease in K was correlated with the finer texture related to the increase in clay percentage. Nevertheless, this evolution differed between the two clay materials tested (Figure 1):

- The NaSwy2-Sand mix can be considered as a waterproof material with K values between 1.35e^{-9} m.s^{-1} (5% clays) and 1.5e^{-12} m.s^{-1} (50% clays)
- The CaSwy2-Sand mix allowed a better percolation at a low clay proportion with K between 4.76e^{-8} m.s^{-1} (5% clays) and 1.11e^{-9} m.s^{-1} (50% clays)

This permeability gap between the two materials can be explained by the differences in physico-chemical clay properties. Whereas the specific surface area and the cationic exchange capacity were similar for both Na- and Ca-Swy2 (Table 2), their macroscopic swelling performance varied greatly impacting their Θ_{max} value.

Injection Pressure	0.1 MPa		0.2 MPa	
Matrix	S	N	S	N
Abbreviation	S1	N1	S2	N2
Q	9	9.1	17.9	18
Filter thickness (mm)	4.39	4.24	4.05	3.95
pH	6.5	6.7	6.5	6.7

with S, the ultra-pure water matrix ; N, the effluent matrix ; Q, the flow in mL.min^{-1} and pH of the initial solution

Table 3 Experimental conditions for percolation experiments with PhACs in solution through a filter composed of 5% of Ca-Swy2 and 95% of Fontainebleau sand

The maximum axial swelling strain ε_{max}, deduced from the measured axial displacements of the piston, revealed a high degree of swelling for the Na-Swy2 smectite compared to Ca-Swy2, 37% and 1.5% respectively (Table 2).

The high swelling capacity of Na-Swy2 influenced the decrease in *K* especially at a low clay percentage (5%). Conversely the extremely low macroscopic swelling for Ca-Swy2 indicates a textural and crystalline swelling control on the decrease in *K*. 5% was the clay proportion selected for the percolation experiments with PhACs in solution.

Ca-Swy2 presents another advantage compared to Na-Swy2 for a field use: the high macroscopic swelling capacity of Na-Swy2 under wet conditions could damage installations which are subjected to dry/wet cycles. While the mechanical behavior of the Ca-Swy2 smectite in association with sand was very similar to non-swelling clay (such as kaolinites) with a low impact of dry/wet cycles, this adsorbent was characterized by a high specific surface area, making it suitable for interaction experiments with emerging organic pollutants.

In view of the very low permeability of the NaSwy2-sand mix, percolation experiments with the PhACs in solution were carried out only with CaSwy2-sand materials as filter. The experimental conditions for the percolation tests with a 5-95% CaSwy2-sand mix are presented in Table 3.

Drug Removal

The global removal of the PhAC pool can be used to estimate the efficiency of the filter in different experimental conditions.

The term C_0 was calculated by the addition of the initial concentrations of the 14 PhACs and C corresponds to the addition of the 14 PhAC concentrations for one collected sample.

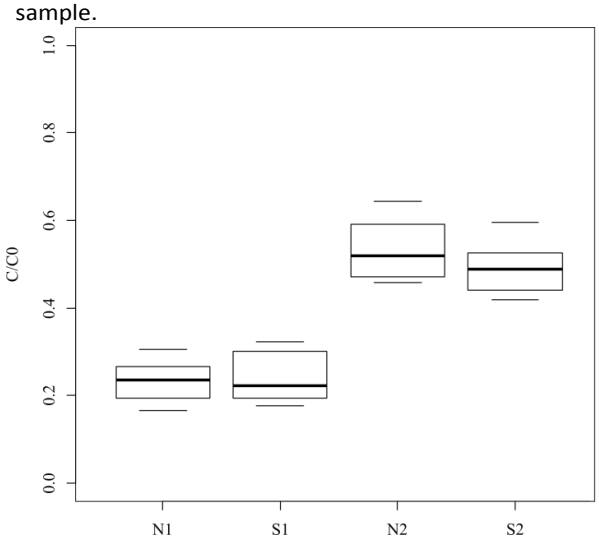

Figure 3: Additive sorption (C/C_0) of all the pharmaceuticals for each experiment: boxes were computed from the removal values added for the 14 pollutants for 10 independent measurements. The line within the box marks the median, boundaries indicate the 25th and 75th percentiles, and error bars indicate the maximum and the minimum removal measurements

The spread of the ten values is around 10% of the total removal (Figure 2) indicating a good regularity in the sorption capacity of the tested material. The adsorption capacity was significant (i.e. > 40%) for all the experimental conditions and the total removal reached was between the extreme values of 35 and 85%. No significant differences in total C/C_0 in the global removal were observed for the two matrices at the same pressure (p = .04 and .06 at 0.1 and 0.2 MPa respectively). The median removal was around 75% at 0.1 MPa and 50% at 0.2 MPa whatever the matrix. The enrichment of the matrix with natural organic matter (NOM) and electrolytes (matrix N) appeared to have no impact on global removal whereas the drop in injection pressure significantly enhanced removal (p<.01 between N1 and N2 and between S1 and S2).

Partition and removal efficiency of targeted PhACs

The solid-liquid distribution coefficient (K_d) is often used to determine the ability of a material to sorb compounds from a solution. This parameter was used to calculate the partition between the solution and the sorbent for each collected sample and estimate its variability between the ten samples for each percolation experiment. Unlike modeling equations of sorption kinetic, the K_d value does not directly depend on the duration of the experiment.

Due to the chosen solid-liquid ratio, PhACs were half-sorbed (50:50) if, Log K_d = 3.40 L.kg^{-1}, and the starting concentration is precisely 25 µg.L^{-1}.

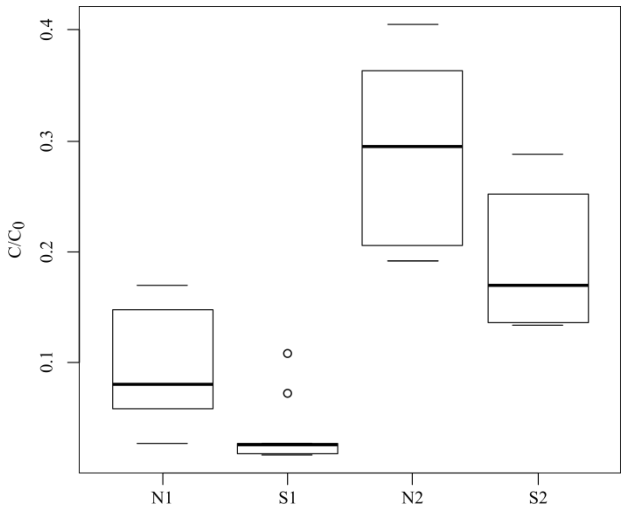

Figure 2: Additive sorption (C/C_0) of the cationic pharmaceuticals for each experiment: boxes were computed from the removal values added for the 14 pollutants for 10 independent measurements. The line within the box marks the median, boundaries indicate the 25th and 75th percentiles, and error bars indicate the maximum and the minimum removal measurements

Cationic Species

Two major trends emerged from the analysis of the total C/C_0 values for the cationic species (Figure 3).

The decrease in the injection pressure, corresponding to a slowdown of the flux was a favorable factor for sorption. For all the compounds, the transition from S2 to S1 was accompanied by a significant increase in the Log K_d (p<.01 for the whole cationic compounds) together with an increase in the total removal (Figure 3).

	S1		N1		S2		N2		onto Sludge
	Log K_d	MRv	Log K_d	MRv	Log K_d	MRv	Log K_d	MRv	Log K_d
Cationic Species									
ATE	4.99 ±0.03	97.0 ± 0.04	4.34 ±0.04	87.6 ± 0.09	3.43 ±0.05	46.2 ± 0.41	3.31 ±0.04	37.2± 0.39	1.58[a]
COD	4.74 ±0.02	95.2 ± 0.03	4.31 ±0.04	88.6 ± 0.11	4.03 ±0.06	73.2 ± 0.24	4.26 ±0.02	86.4± 0.09	1.15[a,b]
DOX	5.79 ±0.01	99.6 ± 0.01	4.86 ±0.02	96.2 ± 0.03	5.38 ±0.01	98.9 ± 0.01	4.57 ±0.02	93.2 ± 0.03	2.14[b]
MET	5.09 ±0.03	96.9 ± 0.03	4.34 ±0.03	89.0 ± 0.08	4.01 ±0.03	77.2 ± 0.16	3.96 ±0.01	75.8 ± 0.12	1.81[b]
TRA	4.63 ±0.03	94.3 ± 0.04	3.96 ±0.04	74.6 ± 0.24	3.94 ±0.02	77.2 ± 0.14	3.65 ±0.02	60.4 ± 0.19	1.67[b]
TRI	4.76 ±0.02	95.3 ± 0.06	4.90 ±0.04	96.4 ± 0.03	4.87 ±0.05	95.0 ± 0.04	4.36 ±0.02	91.4 ± 0.07	1.15[b]
Neutral Species									
DIA	4.20 ±0.03	86.5 ± 0.07	4.19 ±0.03	86.1 ± 0.09	3.45 ±0.04	44.4 ± 0.46	4.33 ±0.04	90.1 ± 0.59	1.72[b]
OXA	3.78 ±0.01	71.6 ± 0.09	3.84 ±0.01	74.4 ± 0.12	2.01 ±0.13	2.0 ± 0.56	3.17 ±0.01	34.4 ± 0.19	1.11[b]
PRO	4.92 ±0.01	97.4 ± 0.01	4.76 ±0.02	96.1 ± 0.03	5.80 ±0.03	99.5 ± 0.01	5.77 ±0.03	99.6 ± 0.01	3.28[a]
Anionic Species									
DCF	3.45 ±0.02	55.3 ± 0.12	3.60 ±0.02	59.8 ± 0.19	2.99 ±0.02	26.2 ± 0.35	3.01 ±0.02	28.9 ± 0.36	1.2[c]
GEM	3.76 ±0.02	71.6 ± 0.09	3.72 ±0.02	67.2 ± 0.18	2.71 ±0.05	13.9 ± 0.72	3.48 ±0.01	52.6 ± 0.16	0.95[a]
IBU	3.07 ±0.02	34.2 ± 0.35	3.35 ±0.01	48.3 ± 0.22	2.08 ±0.04	5.1 ± 0.58	2.61 ±0.04	12.5 ± 0.93	2.23[a]
KET	4.11 ±0.04	81.9 ± 0.03	4.12 ±0.02	84.5 ± 0.09	3.44 ±0.04	40.0 ± 0.56	3.99 ±0.01	79.8 ± 0.05	-
NAP	3.12 ±0.02	40.4 ± 0.29	3.55 ±0.02	53.7 ± 0.41	2.26 ±0.12	6.1 ± 0.86	2.96 ±0.01	24.5 ± 0.27	2.08[a]

with Log K_d in L.kg^{-1}, MRv in %, Relative Standard Deviation values equal to Average/Standard Deviation for n=8 (clipped for the two extreme samples) and values onto sludge from a [42], b [43] and c [44]

Table 4: Log K_d values and Mean Removal values (in %) for selected pollutants ± Relative Standard Deviation for each experiment, compared to Log K_d values found for PhACs onto sludge in the literature

Whereas for the S2 experiment, Log K_d values varied between ATE (3.43) and DOX (5.38), Log K_d values were more homogeneous for the S1 experiment (Table 4). Whatever the injection pressure, the retention of cationic PhACs was generally favored in the case of ultra-pure water (S), except for TRI at 0.1 MPa and COD at 0.2 MPa for which the opposite was recorded. The cationic PhACs were probably in competition with other components (organic or inorganic) contained in the wastewater effluent. As a result, the adsorption of cationic PhACs was lower in matrix N than S (p<.01 for the two injection pressures).

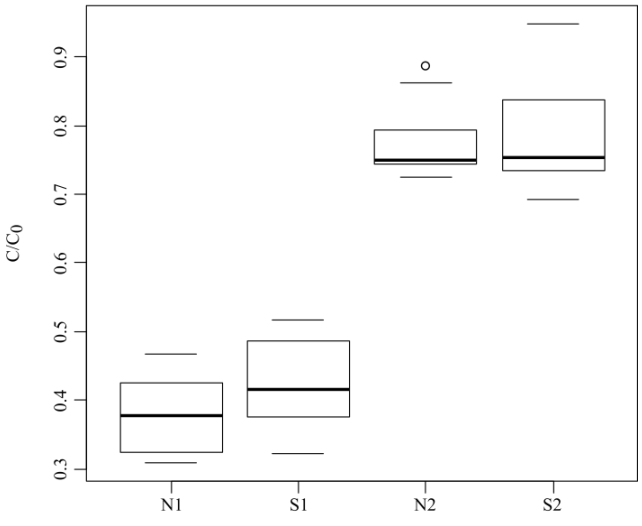

Figure 4: Additive sorption (C/C_0) of the anionic pharmaceuticals for each experiment: boxes were computed from the removal values added for the 14 pollutants for 10 independent measurements. The line within the box marks the median, boundaries indicate the 25th and 75th percentiles, and error bars indicate the maximum and the minimum removal measurements

Anionic species

For anionic PhACs, the shift to a lower injection pressure was also favorable for sorption (Figure 4), especially for IBU in ultra-pure water (S2 vs S1) (Table 4). These results indicated that the interaction kinetic is an important component of the sorption, as for cationic PhACs.

The complexation of the matrix, especially at 0.2 MPa, significantly increased the sorption of all the anionic PhACs (p<.01 at 0.1 and 0.2 MPa). Between S1 and N1, except for IBU, DCF and NAP (e.g. 3.10 to 3.54 respectively), the variations in Log K_d values were not statistically significant (p = .44 and .36 for GEM and KET respectively).

Neutral Species

The solid-liquid distribution variations for the three neutral PhACs did not follow a trend. It was therefore difficult to evaluate the impact of the matrix or of the injection pressure. Whereas PRO was well sorbed whatever the experimental conditions, for DIA and OXA, variations in the Log K_d values were closer to the behavior of anionic species (Table 4).

Partition control factors

The effect of ionic strength or of the presence of organic matter in water, which can favor the sorption of anionic species, was confirmed by the experimental results as suggested in other studies.[45] This assumption can be explained by the adsorption of organic compounds or electrolytes which could enhance the anionic sorption capacities of the clay material.[46]

Kinetic transfer is the second major influence on the sorption capacity. The sorption improvement is particularly strong on anionic species, whose sorption kinetic is known to be slower to reach equilibrium,[47] than that of cationic species (Figure 4).[27]

Measurements of Log K_d values are generally performed onto sludge to better understand the partition of PhACs during waste-water treatment.[42–44] Thus, sorption on sludge can be considered as a removal despite the

variable further use of sludge. If we compare the Log K_d values onto secondary sludge in the literature for each compound (Table 4), there is no link between the charge of the pollutant and the Log K_d. IBU or NAP are well sorbed onto sludge whereas other anionic compounds have a Log K_d < 2. These compounds were also among the three anionic compounds to be significantly better sorbed in N matrix than S (Table 4) at 0.1 MPa. The combination of these two factors demonstrated the NOM impact on the sorption of some anionic PhACs.

For cationic species, only one value (for DOX) exceeds 2 and only the neutral compound PRO is well sorbed by sludge.

The affinity of our material with PhACs was far greater than that of sludge, with Log K_d values up to at least for the N1 experiment, indicating that the chosen material has better trapping properties than sludge.

The greater complexity of sludge in terms of chemical reactivity results in a variable affinity with the targeted PhACs that does not depend only on the charge of the pollutants,[48] whereas with clay material, the charge seems to play the most important role in the control of sorption.

Sorption kinetics modeling

Based on the obtained correlation coefficients of the three models tested that spread out from 0.90 to 0.999 (Tables S3, S4 and S5), it appears that the experimental data are better adjusted with Bangham equation (r^2 comprised between 0.970 and 0.999). Nevertheless, the whole models used here provide similar trends. The efficiency of the adsorption is enhanced at high pressure as shown by k_1 constants (first-order Lagergen). Figures 5 and 6 confirm and highlights the sorption rate was higher at 0.2 MPa than at 0.1 MPa indicating a better sorption efficiency at higher kinetic percolation.

The second-order Lagergren (Table S4) and Bangham (Table S5) equations suggested a good regularity of the removal quality of the material as Log K_d standard deviation values expressed.

For the best sorbed compounds DOX, PRO and TRI, the comparison of k_2 and q_m values indicated the same trends as those observed with the Log K_d analysis on the matrix effect. An increase in log k_2 corresponding with a drop in q_m between respectively S and N (for each injection pressure) indicated a matrix effect that was unfavorable for the adsorption of cationic compounds.

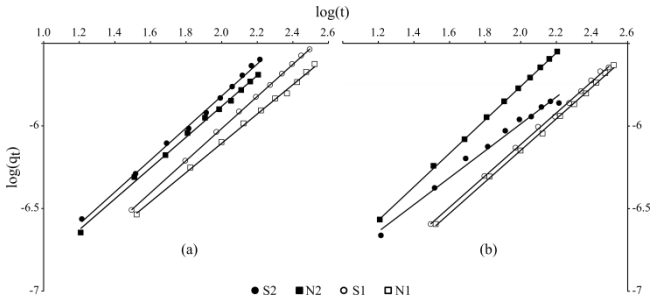

Figure 5: Bangham fits (solid lines) for (a) Tramadol (cationic) and (b) Ketoprofen (anionic) for each experiment

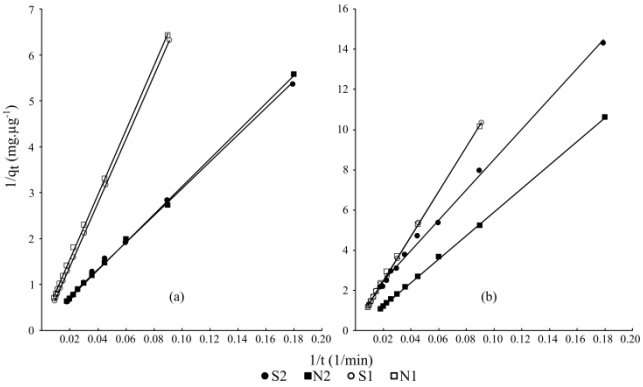

Figure 6: Pseudo second-order fits (solid lines) for (a) Metoprolol (cationic) and (b) Diazepam (neutral) for each experiment

The exact opposite was observed for IBU, OXA and NAP, with a lower log k_2 and a higher q_m for N than S. For the other compounds, the data can be interpreted as shown in Figure 5. For cationic species, there was a slight unfavorable effect of the N matrix whereas the opposite was observed for anionic species.

Unlike the Log K_d values, the modeling and resulting sorption efficiency values gave contrasting results. The main controlling factor for the sorption capacity of Ca-Swy2 towards PhACs is the chemical properties of the molecule. As this material has a greater cationic than anionic exchange capacity, cationic compounds were strongly favored for sorption.

Otherwise, the sorption of anionic compounds was slightly better in effluent matrix than in ultra-pure water but it remained significantly lower than for cationic compounds. This enhancement of anionic species adsorption by the addition of NOM or electrolytes has already been reported for IBU alone onto montmorillonite, indicating that without a saturation effect, the behavior of a pool of PhACs with Ca-Swy2 is similar to that of a single PhAC.

Model fittings demonstrated that Ca-Swy2 has a large sorption capacity spectrum even if the molecular charge remained a key factor for the removal ratio.

While the better removal efficiency at a lower injection pressure seemed to improve sorption, modeling results showed that the sorption rate was higher for higher injection pressures. With a view to optimizing the kinetic transfer through the filter, further data need to be obtained to combine the best removal efficiency with the best sorption rate constant.

Clays characterization

Clays were separated from sand after the leachate test for further characterization. Two methods were applied to investigate the adsorbent reaction to the leachate, XRD and FTIR analysis.

XRD and FTIR exhibited no significant layer expansion or band stretching respectively after experiments.

Elemental analyses were carried out on the clay minerals after the percolation of 1 liter in order to estimate the

total sorbed concentration based on the carbon percentage of the clays (Figure 7).

The comparison between elemental analyses on clays and leachate sample analyses exhibited similar results for the ultra-pure water matrix. This is consistent with the assumption that clays are responsible for most of the sorption in comparison with sand. Similar results between clays and water samples also indicated that PhACs are effectively adsorbed onto Ca-Swy2 and not degraded furthermore.

In accordance with previous results obtained from solution analyses, the total sorbed concentration was higher for S1 than S2, with a total removal of 65.7% and 48.2% respectively.

For N matrices, the elemental analysis results are significantly higher than those of the leachate samples. This indicates that the material adsorbed more than PhACs from the effluent matrix. The additional organic compounds that were adsorbed may possibly explain the better sorption for anionic compounds in the effluents.[49]

Sorption Mechanisms

Despite the excellent removal efficiency of the prepared mineral mixture in this study, sorbed PhACs amounts remain low due to the selected starting concentrations that were 25 $\mu g.L^{-1}$. Since the sorbed amounts for the whole PhACs were rather low, it was rather hard to probe any changes through the use of classical analytical techniques such as FTIR or XRD, which may acknowledge us about conformation of molecules and their localization for a proper description of the adsorption processes.

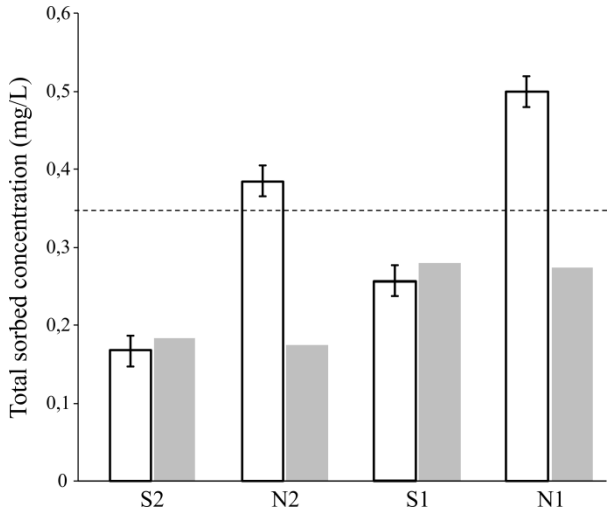

Figure 7: Comparison between the total sorbed concentrations calculated by elemental analysis of clays (white bars) and from the leachate samples (gray bars) for each percolation test. The dotted line corresponds to the total injected concentration of PhACs

Nevertheless, it appears that the sorption of anionic PhACs is particularly enhanced for clay mineral with Ca^{2+} as compensating cations. Indeed, Ca^{2+} is divalent and showed its ability to sorb anionic species by cationic bridges.[50] Here, the results suggest a better sorption efficiency of anionic species in contrast to previous studies using sodium exchanged Na-Swy2.[49,51] However electrostatic interactions or even hydrogen bonds cannot be excluded that may play also as driving forces for the adsorption. Further experiments need to be carried out to better point out the sorption mechanisms.

Cationic species are usually adsorbed on clay mineral through cation exchanges and it may also the case for PhACs here. This mechanism is thermodynamically spontaneous,[27] but only compensating cations on the external surfaces are involved since no changes in the diffraction patterns were observed.

Conclusions

From the results of this study, the following conclusions can be drawn:

- Natural Ca-saturated smectite (Ca-Swy2) incorporated into a sand-filter allowed a flow consistent with *in-situ* applications whereas Na-saturated smectite (Na-Swy2) is a waterproof material that is not adapted to the sorption of pollutants in a simulation of dynamic sorption close to field reality
- Ca-Swy2 exhibited a large adsorption capacity even for cationic, neutral and anionic PhACs at similar wastewater pH. With the values of the relative standard deviation of samples, it seems that the sorption efficiency in time is steady. The sorption capacity is guided by two major parameters, infiltration kinetics and the composition of the matrix.
- The effluent matrix played a contrasting role on the sorption efficiency, depending on the molecular charge and the speciation at the tested pH: anionic species were favored by this complex matrix in contrast to cationic ones, for which the sorption efficiency was lower. Some NOM and/or electrolytes of the effluent were also adsorbed onto the filter and played a key role in the sorption of anionic compounds whereas they were in competition with cationic species. Further analyses need to be carried out to characterize them.
- The applied models fitted our data well, but due to the pseudo equilibrium that was reached, the calculated constants did not correspond to previous observations for all the models. However, even a low kinetic (0.1 MPa) favored sorption processes, and at higher injection pressure sorption processes were more efficient

- Natural Ca-smectite is a slightly modified material that could significantly improve the removal efficiency of current treatment chains, especially concerning the removal of PhACs.
- The key role played by the interlayer cation can direct the choice of geosorbent for further studies, using clays minerals that are naturally saturated by Ca^{2+}, rather than by Na^{+}
- Implementation in the field of the tertiary treatment technique presented here requires further experiments. Nevertheless, this study stresses out the relevance of the material in a field application for a good removal efficiency especially in comparison with tertiary treatments using chemical products, potentially toxic for the environment. The main question now is the management costs induced by this technique, especially concerning the durability of the filter.

Acknowledgements

The work received financial support from the HArPE Project (2012-00073536) funded by the Région Centre-Val de Loire. The authors would also like to thank Fabrice Muller for XRD and FTIR analysis and Marielle Hatton for carbon analysis.

Notes and references

1 C. G. Daughton and T. A. Ternes, *Environ. Health Perspect.*, 1999, **107**, 907.
2 A. Masiá, J. Campo, P. Vázquez-Roig, C. Blasco and Y. Picó, *J. Hazard. Mater.*, 2013, **263, Part 1**, 95–104.
3 T. Heberer, *J. Hydrol.*, 2002, **266**, 175–189.
4 R. Loos, B. M. Gawlik, G. Locoro, E. Rimaviciute, S. Contini and G. Bidoglio, *Environ. Pollut.*, 2009, **157**, 561–568.
5 M. L. Richardson and J. M. Bowron, *J. Pharm. Pharmacol.*, 1985, **37**, 1–12.
6 T. A. Ternes, *Water Res.*, 1998, **32**, 3245–3260.
7 T. Heberer, *Toxicol. Lett.*, 2002, **131**, 5–17.
8 B. F. da Silva, A. Jelic, R. López-Serna, A. A. Mozeto, M. Petrovic and D. Barceló, *Chemosphere*, 2011, **85**, 1331–1339.
9 P. Vazquez-Roig, V. Andreu, C. Blasco and Y. Picó, *Sci. Total Environ.*, 2012, **440**, 24–32.
10 M. S. Kostich, A. L. Batt and J. M. Lazorchak, *Environ. Pollut.*, 2014, **184**, 354–359.
11 P. Cardinal, J. C. Anderson, J. C. Carlson, J. E. Low, J. K. Challis, S. A. Beattie, C. N. Bartel, A. D. Elliott, O. F. Montero, S. Lokesh, A. Favreau, T. A. Kozlova, C. W. Knapp, M. L. Hanson and C. S. Wong, *Sci. Total Environ.*, 2014, **482–483**, 294–304.
12 X. Li, W. Zheng and W. R. Kelly, *Sci. Total Environ.*, 2013, **445–446**, 22–28.
13 R. Loos, R. Carvalho, D. C. António, S. Comero, G. Locoro, S. Tavazzi, B. Paracchini, M. Ghiani, T. Lettieri, L. Blaha, B. Jarosova, S. Voorspoels, K. Servaes, P. Haglund, J. Fick, R. H. Lindberg, D. Schwesig and B. M. Gawlik, *Water Res.*, 2013, **47**, 6475–6487.
14 K. Fent, A. A. Weston and D. Caminada, *Aquat. Toxicol.*, 2006, **76**, 122–159.
15 Â. Almeida, R. Freitas, V. Calisto, V. I. Esteves, R. J. Schneider, A. M. V. M. Soares and E. Figueira, *Comp. Biochem. Physiol. Part C Toxicol. Pharmacol.*, 2015, **172–173**, 26–35.
16 T. Brodin, J. Fick, M. Jonsson and J. Klaminder, *Science*, 2013, **339**, 814–815.
17 N. Casatta, G. Mascolo, C. Roscioli and L. Viganò, *Sci. Total Environ.*, 2015, **511**, 214–222.
18 K. Grabicova, R. H. Lindberg, M. Östman, R. Grabic, T. Randak, D. G. Joakim Larsson and J. Fick, *Sci. Total Environ.*, 2014, **488–489**, 46–50.
19 C. M. de Jongh, P. J. F. Kooij, P. de Voogt and T. L. ter Laak, *Sci. Total Environ.*, 2012, **427–428**, 70–77.
20 J. Altmann, A. Sperlich and M. Jekel, *Water Res.*, 2015, **84**, 58–65.
21 M. Klavarioti, D. Mantzavinos and D. Kassinos, *Environ. Int.*, 2009, **35**, 402–417.
22 I. Ali, M. Asim and T. A. Khan, *J. Environ. Manage.*, 2012, **113**, 170–183.
23 S. M. Lee and D. Tiwari, *Appl. Clay Sci.*, 2012, **59–60**, 84–102.
24 R. Guégan, M. Giovanela, F. Warmont and M. Motelica-Heino, *J. Colloid Interface Sci.*, 2015, **437**, 71–79.
25 G. Z. Kyzas, J. Fu, N. K. Lazaridis, D. N. Bikiaris and K. A. Matis, *J. Mol. Liq.*, 2015, **209**, 87–93.
26 T. Polubesova, D. Zadaka, L. Groisman and S. Nir, *Water Res.*, 2006, **40**, 2369–2374.
27 P.-H. Chang, W.-T. Jiang, Z. Li, C.-Y. Kuo, J.-S. Jean, W.-R. Chen and G. Lv, *J. Hazard. Mater.*, 2014, **277**, 44–52.
28 A. Mahamat Ahmat, M. Boussafir, C. Le Milbeau, R. Guegan, J. Valdès, M. Guiñez, A. Sifeddine and L. Le Forestier, *Mar. Chem,* 2016, **179**, 23-33.
29 S. Zheng, Z. Sun, Y. Park, G. A. Ayoko and R. L. Frost, *Chem. Eng. J.*, 2013, **234**, 416–422.
30 T. Thiebault, R. Guégan and M. Boussafir, *J. Colloid Interface Sci.*, 2015, **453**, 1–8.
31 I. Aksu, E. Bazilevskaya and Z. T. Karpyn, *GeoResJ*, 2015, **7**, 1–13.
32 L. Wu, L. Liao and G. Lv, *J. Colloid Interface Sci.*, 2015, **454**, 1–7.
33 L. Le Forestier, F. Muller, F. Villieras and M. Pelletier, *Appl. Clay Sci.*, 2010, **48**, 18–25.
34 A. Jullien, C. Proust, L. Le Forestier and P. Baillif, *Appl. Clay Sci.*, 2002, **21**, 143–153.
35 M. Gautier, F. Muller, L. Le Forestier, J.-M. Beny and R. Guegan, *Appl. Clay Sci.*, 2010, **49**, 247–254.
36 C. Schummer, O. Delhomme, B. M. R. Appenzeller, R. Wennig and M. Millet, *Talanta*, 2009, **77**, 1473–1482.
37 M. Carballa, G. Fink, F. Omil, J. M. Lema and T. Ternes, *Water Res.*, 2008, **42**, 287–295.
38 L. Yang, M. Jin, C. Tong and S. Xie, *J. Hazard. Mater.*, 2013, **244–245**, 77–85.
39 P. A. Domenico and F. W. Schwartz, *Physical and chemical hydrogeology*, Wiley, New York, NY, 2. ed., 1998.
40 F. T. Madsen, *Clay Miner.*, 1998, **33**, 109–129.
41 M. Ghayaza, L. Le Forestier, F. Muller, C. Tournassat and J.-M. Beny, *J. Colloid Interface Sci.*, 2011, **361**, 238–246.
42 B. Blair, A. Nikolaus, C. Hedman, R. Klaper and T. Grundl, *Chemosphere*, 2015, **134**, 395–401.
43 A. Wick, G. Fink, A. Joss, H. Siegrist and T. A. Ternes, *Water Res.*, 2009, **43**, 1060–1074.

716 44 T. A. Ternes, N. Herrmann, M. Bonerz, T. Knacker, H. Siegrist
717 and A. Joss, *Water Res.*, 2004, **38**, 4075–4084.
718 45 T. X. Bui and H. Choi, *Chemosphere*, 2010, **80**, 681–686.
719 46 H. Mansouri, R. J. Carmona, A. Gomis-Berenguer, S. Souissi-
720 Najar, A. Ouederni and C. O. Ania, *J. Colloid Interface Sci.*,
721 2015, **449**, 252–260.
722 47 V. Calisto, C. I. A. Ferreira, J. A. B. P. Oliveira, M. Otero and V.
723 I. Esteves, *J. Environ. Manage.*, 2015, **152**, 83–90.
724 48 M. Hörsing, A. Ledin, R. Grabic, J. Fick, M. Tysklind, J. la C.
725 Jansen and H. R. Andersen, *Water Res.*, 2011, **45**, 4470–4482.
726 49 S. K. Behera, S. Y. Oh and H. S. Park, *Int. J. Environ. Sci.*
727 *Technol.*, 2012, **9**, 85–94.
728 50 E. Errais, J. Duplay, M. Elhabiri, M. Khodja, R. Ocampo, R.
729 Baltenweck-Guyot and F. Darragi, *Colloids Surf. Physicochem.*
730 *Eng. Asp.*, 2012, **403**, 69–78.
731 51 J. Gao and J. A. Pedersen, *Environ. Sci. Technol.*, 2005, **39**,
732 9509–9516.
733